Available online at www.sciencedirect.com
ScienceDirect
Trans. Nonferrous Met. Soc. China 33(2023) 1873−1892
Transactions of Nonferrous Metals Society of China
www.tnmsc.cn

Geochemistry and petrogenesis of rare-metal pegmatites: A case study of Lemera Sn ore deposits in Kivu region of Karagwe-Ankole Belt, D. R. Congo

Rub'son N'nahano-Ruhindwa HERITIER[1,2], Moïse LUEMBA[3,4], Huan LI[1], Charles NZOLANG[5], Donat KAMPATA[4,6], Joseph NTIBAHANANA[3,4,7]

1. Key Laboratory of Metallogenic Prediction of Nonferrous Metals and Geological Environment Monitoring, Ministry of Education, School of Geosciences and Info-physics, Central South University, Changsha 410083, China;
2. State Key Laboratory of Geological Processes and Mineral Resources, China University of Geosciences, Beijing 100083, China;
3. School of Geosciences, China University of Petroleum (East China), Qingdao 266580, China;
4. Faculty of Oil, Gas and New Energies, University of Kinshasa, B. P. 127 Kinshasa XI, D. R. Congo;
5. Official University of Bukavu, Bukavu, South Kivu, D. R. Congo;
6. National Geological Service, Ministry of Mines, Kinshasa, D. R. Congo;
7. Geophysical Research Center, Ministry of Research and Technological Innovation, Kinshasa, D. R. Congo

Received 29 January 2022; accepted 15 August 2022

Abstract: This paper reports the results from an investigation on petrogenesis and geochemistry of the Lemera granite pegmatites in Kivu region of Karagwe-Ankole Belt, D. R. Congo and the related tin ore deposits. Seven granite pegmatite samples were collected from outcrops and analyzed for bulk-rock geochemistry analysis using ICP-MS and XRF spectrometry. The analyzed samples show a relative abundance of Al_2O_3 over Fe_2O_3(T) and MgO (12.95, 0.96, and 0.16, all in wt.%, on average and respectively). The alumina saturation index ranges from 1.33 to 2.05. The abundances of some important rare metals, as well as some related key parameters, are as follows: Sn ((1−138)×10^{-6}), Ta ((0.20−0.60)×10^{-6}), Nb ((1−8)×10^{-6}), Cs ((1.20−3.20)×10^{-6}), Rb ((3−223)×10^{-6}), Zr ((7−201)×10^{-6}), w(K)/w(Rb) (150−272); w(K)/w(Cs) (9.06−23.3); w(Nb)/w(Ta) (3.33−14). The results indicate that the Lemera granite pegmatites crystallized from a fertile, peraluminous, and S-type granitic magma through a fractional crystallization process in a late to post-collisional setting. Mineralization of Sn and Zr of Lemera granite pegmatites is noticed.
Key words: Kibaran Belt; Lemera granite pegmatites; tin ore deposits; S-type granites; fractional crystallization

1 Introduction

Pegmatites are highly coarse-grained crystalline rocks that, in certain locations, include gigantic crystals of quartz, feldspar, or mica, making this felsic lithology stand out from the compositionally identical granites [1,2]. The Karagwe-Ankole Belt shows a co-occurrence of Sn−W quartz vein-type and Nb−Ta−Sn pegmatite- type mineralization at several locations, which is a rare opportunity for the investigation of the geochemical evolution and elemental distribution throughout the transition from magmatic to hydrothermal processes. Several studies were conducted in the Karagwe-Ankole Belt, which resulted in the proposal of models regarding its tectono-magmatism and Nb−Ta−Sn−W metallogeny, including the geochronological

Corresponding author: Huan LI, Tel: +86-731-88877151, E-mail: lihuan@csu.edu.cn
DOI: 10.1016/S1003-6326(23)66229-6

information of each magmatism and mineralization, as well as the structural influence. Two sets of models have been proposed regarding the tectonic context related to each magmatism. The first model suggested that the region was in an intracratonic environment with the most significant anorogenic event occurring at 1375 Ma and a compressional deformation occurring at 1000 Ma, which is thought to be an Irumide Orogen far-field effect [3,4]. The Karagwe-Ankole Belt, on the other hand, is interpreted by the second set of models as an active margin associated with the Tanzania/ Bangweulu Block-Congo Craton convergence around 1375 Ma [5−7]. A recent study of the granitic rocks of the Karagwe-Ankole Belt has provided evidence pointing to tectonic evolution of the belt during accretion-collisional tectonism [8], which led to a more plausible tectono-magmatic model that places the emplacement of anorogenic garnet-biotite granite (A-type granite) at (1372±5) Ma, followed by a group of orogenic granites (S-type granite), including two-mica granites that were emplaced at (1369±5) Ma, late to post-collisional muscovite granite and leucogranite ((1011±18) Ma to (976±11) Ma), and a younger leucogranite ((614±9) Ma) related to a volcanic arc setting. These S-type muscovite granites and leucogranites obviously constitute the widely documented G_4 granitoids that were reported by KLERKX et al [9], CAHEN et al [10], FERNANDEZ-ALONSO et al [11] and TACK et al [12].

In addition, some metallogenic studies conducted in the belt suggest that the Kibaran Sn granites (the above-cited muscovite granite and leucogranite), the Nb−Ta−Sn pegmatites, and the Sn−W quartz veins evolved spatiotemporally as one integrated metallogenic system operated at (980±20) Ma [13−19]. A recent study has reported three generations of Sn mineralization, based on SHRIMP U−Pb dating of cassiterite [20]. The cited study reported that the first generation occurred in pegmatite (1145 Ma), while the second generation and main mineralization occurred in quartz veins and intra-pegmatitic greisen (1090−960 Ma), followed by the third generation occurring in quartz veins (530 Ma). It is noted that debates are still ongoing among researchers regarding the role played by magmatic fluid in carrying the metals during magma evolution [21,22]. Despite the fact that tin mineralization has been experimentally recognized to have a magmatic source [23], the direct relationship between ore mineralization and granitic formation remains a mystery in central Africa. Some studies proposed that the tin mineralizing veins are the result of crystalline aliquots of the escaping evolved fluids from the magmatic-pegmatite systems [18,24]. In contrast, other authors reported that the Sn metal was taken by the metamorphic hydrothermal fluids from the magmatic rocks after crystallization [25,26].

Although there are several Proterozoic Sn deposits under development in the Kibaran Belt (Karagwe-Ankole and Kibara Belts) (Fig. 1), particularly in the eastern D. R. Congo, only a few researchers have focused on the petrogenesis and geochemistry of pegmatites and their associated Sn ore deposits in the Kivu region [27−30]. The purpose of this investigation is to categorize the Lemera granite pegmatites in order to understand their genesis and evolution during the magmatic fractionation, and put their mineralization potential into evidence. We expect, at the end, to provide the genetic link between the tin ore deposits, which are quartz vein-types and the pegmatite-type, with respect to the regional G_4 granites (muscovite granite and leucogranite) and the nature of the ores carrying fluid.

2 Geological setting of Kibaran Belt

The Kibaran Belt refers to the Meso-proterozoic Fold Belt, including the Kibara Belt (KIB) and the Karagwe-Ankole Belt (KAB) (Fig. 1(a)) [4]. From north to south, the African continent was shaped by three large Archean cratons: the West-African Craton, the Congo Craton, and the Kalahari Craton, all of which are illustrative of an epoch older than 2500 Ma (Fig. 1(b)). When these three crustal nuclei were assembled during the reconstruction period, they provided clues to the formation of the main fold belts that formed from the Proterozoic to the early Paleozoic epochs. The Ubende Belt and the Ruzizi Belt in Central Africa represent the Paleoproterozoic (approximately 2000 Ma), whereas the Kibaran Belt (including the Karagwe-Ankole Belt and the Kibara Belt) in East-Central Africa and the Kamativi Belt in Zimbabwe expose the Mesoproterozoic rocks. The KAB is divided into two distinct structural domains:

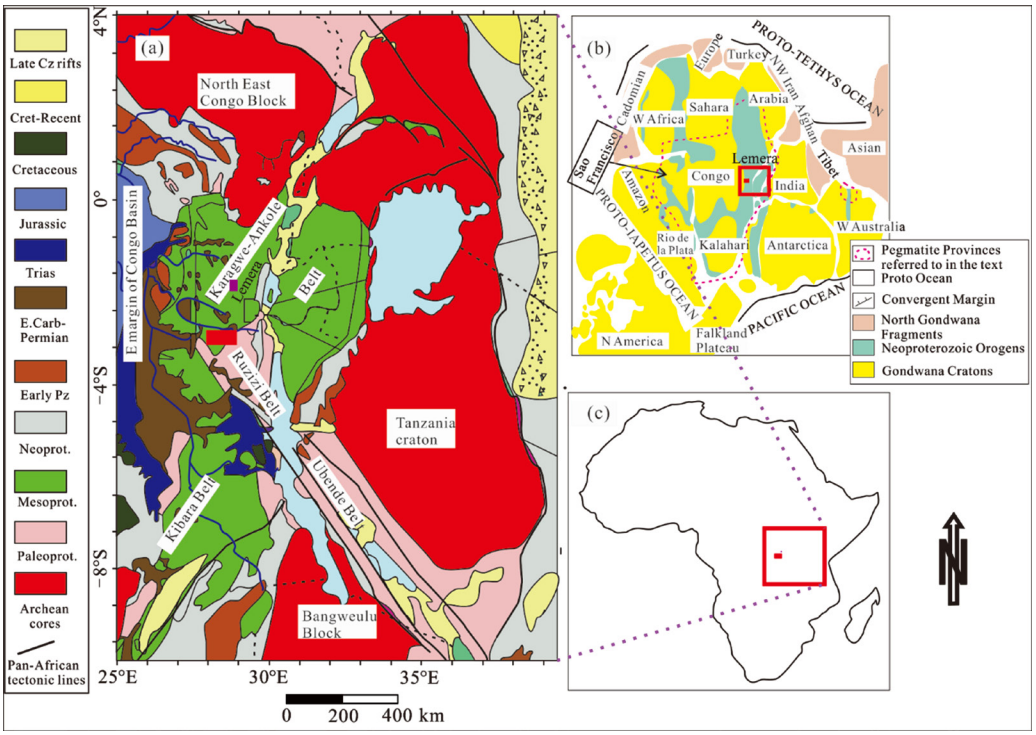

Fig. 1 (a) Schematic geodynamic map of Kivu region (modified from DELVAUX et al [13]); (b) Schematic map of reconstructed Gondwana plate showing documented pegmatite provinces (modified from DILL [2] and KUSKY et al [14]); (c) Approximate location of Lemera area on map of Africa

the western domain (WD) and the eastern domain (ED), which are separated by a boundary zone of aligned mafic-ultramafic layered complexes known as the Kabanga-Musongati alignment [8,30]. A recent study has reported the discovery of Neoarchean crust within the Rusizian terrane of the western domain of the KAB and suggested consideration of an Archean basement in the cited location [30]. The Pan-African Orogeny refers to the following belts: the Damara Belt in Namibia; the Arabo-Nubian Shield in the northeast of Africa; and the Mozambique Fold Belt in the southeast of Africa. All these belts were formed in the late Neoproterozoic to early Paleozoic at (600−450) Ma (Fig. 1(a)) [2,5,13]. Kibaran Belt (Mesoproterozoic) separates the Congo Craton (Archean-Paleoproterozoic) from the Bangweulu-Tanzania Block (Archean-Paleoproterozoic) (Fig. 1(a)). At 1375 Ma and approximately 1000 Ma, widespread magmatism occurs throughout this region [5,8,31]. The (1417−1376) Ma magmatic events are usually regarded as an active continental margin in the southwestern part (Kibara Belt) [5,8,31,32], whereas an intracratonic basin was hypothesized for the northeastern part (Karagwe-Ankole Belt) [8,9,33]. The evolution of the Mesoproterozoic Karagwe-Ankole Belt has been recently re-constrained with multiple stages of magmatism from subduction to collision [8]. As a result, its evolution is proven to have occurred during the accretion-collision tectonism in a continental margin.

The Kibaran Belt is mainly composed of metasedimentary units, mostly metamorphosed pelites, conglomerates and sandstones with minor carbonate rocks. Large felsic and mafic rocks have intruded these metasedimentary units [10].

The Lemera district is located in the Uvira territory, South-Kivu province (eastern part of the D. R. Congo) (Fig. 2). The geological units of Lemera are mainly composed of metamorphic rocks (gneiss, migmatite, quartzites and schist) intruded by granitoids (granites and pegmatites). The granites, pegmatites, and aplites occur as dykes and do not appear easily on the surface as an outcrop. The granites intruded gneissic rocks, which were altered and crossed by numerous quartz veins. The veins were measured from 1 to 50 cm in width. The main rocks in the region were subjected to at least two phases of deformation, and the mineralization was confined to folds plunging very shallowly

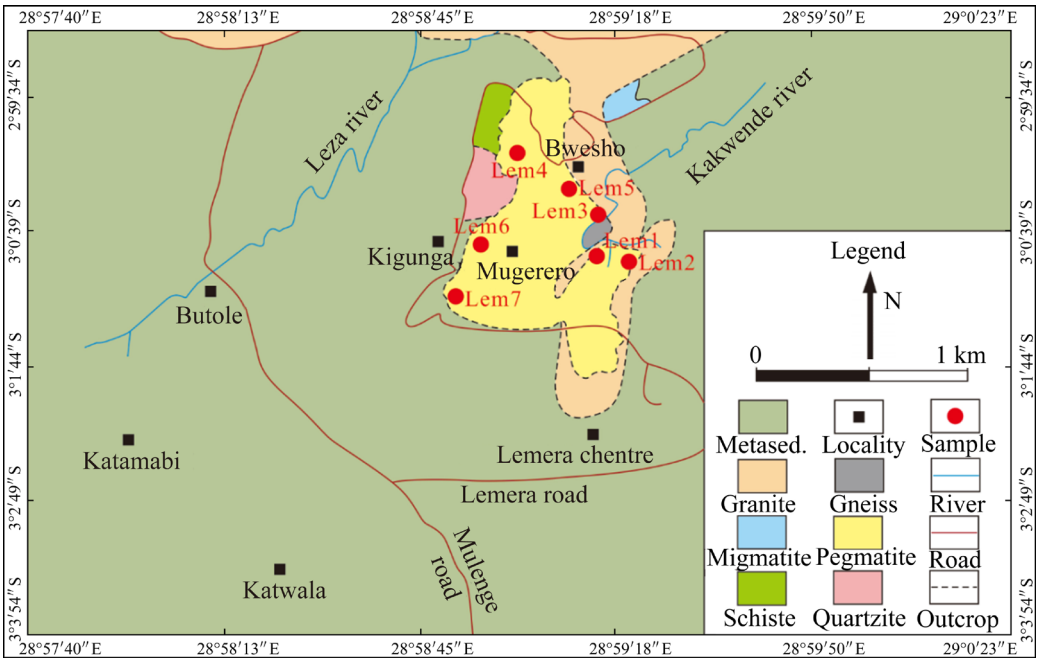

Fig. 2 Schematic geological map of Lemera area

towards the N23°E. The Lemera tin deposit was discovered in 2008, and the main mineral yet exploited is cassiterite, which is mined by local people involved in artisanal mining operations within the strongly phyllitic alteration zone situated adjacent to granite pegmatites.

The large metallogenic provinces hosted by the Kibaran Belt are located in or adjacent to the G_4 tin granites bearing the main metals of Sn−Ta−Nb−W polymetallic deposits. These rare metals are present in different styles of mineralization. Primarily, the mineralization occurs in quartz veins, lodes, and pegmatites, and the secondary mineralization is present in alluvial and illuvial deposits [20,25,26]. The G_4 tin granites are typically non-foliated and include both leucogranites and muscovite granites with quartz, albite, and muscovite as major minerals, adding to them the accessory minerals of apatite, garnet, zircon, and tourmaline. The G_4 tin granites have a fractionation trend character with a generally sub-alkaline to peraluminous modal distribution [20,34]. The main enrichments displayed by most G_4 granitoids are Li, Rb, Cs, U, B, Ga, Ge, Sn, and Pb [35]. The largest Ta−Nb−Sn−W provinces are situated in the zoned pegmatites and unzoned pegmatites with different size types where much of the Sn mineralization is more abundant in the greisen zones and hydrothermal quartz veins [25].

The study in Ref. [27] is one of the rare research works conducted in the region, which reported an important enrichment in Ta ((27.50−370.90)×10^{-6}), Sn ((238−2451)×10^{-6}) and Nb ((31.80−139.20)×10^{-6}) from the Numbi pegmatite samples (Kalehe Territory, South Kivu Province, D. R. Congo). It is worth noting that the majority of the studies mentioned in the preceding paragraphs were conducted in the Gatumba area of Rwanda, which includes a well-developed pegmatite field; thus, the Gatumba pegmatites are the most studied and documented pegmatites in Central Africa [18,28−30].

NAMBAJE et al [20] classified the Sn mineralization in the KAB into four types: (1) Sn mineralization takes place in quartz veins within micaschists, primarily within shear zones, which characterize the majority of the recorded mineralization; (2) Sn mineralization in quartz veins that are restricted to quartzites and are structurally regulated by faults in the host rocks; (3) Mineralization of feldspar in intra-pegmatitic greisen, which is abundant in the zone of contact between pegmatite and amphibolite; (4) Sn mineralization in kaolinized pegmatites intermingled with Nb−Ta mineralization in pegmatites that host Sn deposits and are more closely related to granitic plutons than the quartz vein deposits.

3 Samples and methods

The samples analyzed in this work were collected from pegmatite outcrops within the Lemera area, precisely along the Kakwende River, the Kigunga road, and the Bwesho hill (Fig. 2). Some representative photographs of the Lemera granite pegmatites are presented in Fig. 3. Seven samples were analyzed for bulk-rock major geochemical composition. On fused glass beads, XRF spectrometry was applied for the detection and quantitation of major, minor, and some trace elements in bulk-rock samples at Kyungpook National University (Petrology and Mineralogy Laboratory) using the Rigaku RIX 3000 system. The beads were made by combining 1.8 g of rock powder with 2.88 g of lithium tetra-borate ($Li_2B_4O_7$) and 0.72 g of lithium metaborate ($LiBO_2$), plus 0.05 g of 4.5% Li−Br solution.

Moreover, an inductively coupled plasma-mass spectrometry (ICP-MS) experiment was conducted at Activation Laboratories Ltd (Actlabs) in Canada. This experiment was applied for the detection and quantification of rare earth elements (REE) and trace elements, using the Agilent Series 7500. Approximately 0.05 g of sample powder was dissolved in solutions of HF + $HClO_4$ and then HF doped HNO_3 + HCl through a series of heating and evaporation stages to produce the sample. The solution was diluted by a factor of 50000 after full dissolution.

Aiming at constraining the relationship among the Lemera granite pegmatites, the G_4 granites (Kibaran Belt), the muscovite granites and the leucogranites (Karagwe-Ankole Belt/Rwanda), representative bulk-rock compositions were collected from NAMBAJE et al [8], LEHMANN and LAVREAU [34], and POHL and GÜNTHER [36]. In addition, only seven representative samples of the G_4 granite were selected from the following sites: Bukena, Kalima, Kirengo, Lutshuruk, Madyakala, Makamba, and Mts Bia; while the S-type muscovite granites and the leucogranites were all selected from Rwandan sites in the Karagwe-Ankole Belt.

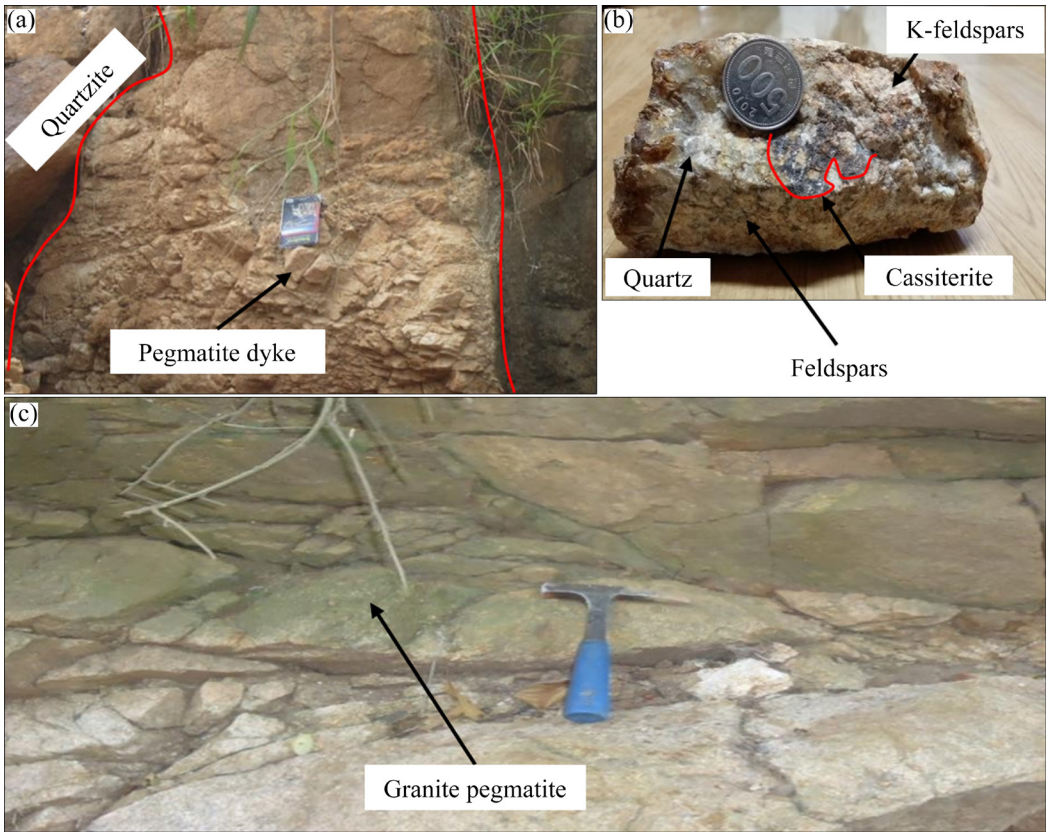

Fig. 3 Photographs of Lemera granite pegmatites: (a) Giant dyke of LCT granite pegmatites; (b) Hand specimen of Lemera granite pegmatites; (c) Intrusion of granite pegmatites into meta-schist rocks along Kakwende River

4 Results

4.1 Bulk-rock major oxides, classification and origin of Lemera granite pegmatites

The distribution of the whole-rock major oxides, expressed in mass fraction, of the analyzed Lemera granite pegmatites samples is presented in Table 1. The total alkali silica (TAS) diagram for plutonic rock classification shows that the Lemera pegmatites are in the range of granite [37], the same range as the G_4 granites that are representative of tin-bearing granites in the Kibaran Belt and the data were collected from LEHMANN and LAVREAU [34], and POHL and GÜNTHER [36] (Fig. 4(a)).

Furthermore, plotted on a ternary diagram of Fe_2O_3 (T), MgO, and Al_2O_3, after RAHMAN [38], all the samples fall into the field of S-type granites (Fig. 4(b)). In the same way, the alumina saturation index (A/CNK) of the Lemera granite pegmatites ranges within 1.33−2.05, which confirms that these granitic pegmatites crystallized from a mildly to strongly peraluminous and fertile granitic melt (A/CNK>1.0).

In addition, the plot of Fe_2O_3 content and the silica differentiation index displayed a negative correlation from the G_4 granites to the less evolved

Table 1 Bulk-rock major oxide distribution in Lemera granite pegmatites (all detected by XRF spectrometry) (wt.%)

Major oxide	LEM1	LEM2	LEM3	LEM4	LEM5	LEM6	LEM7	Min.	Mean	Max.
SiO_2	73.84	76.42	73.82	73.04	76.82	82.1	80.14	73.04	76.60	82.10
Al_2O_3	13.58	13.19	15.8	16.38	12.13	9.1	10.48	9.10	12.95	16.38
MgO	0.18	0.18	0.31	0.07	0.06	0.15	0.16	0.06	0.16	0.31
Fe_2O_3(T)	0.88	0.84	0.69	0.51	0.56	1.27	1.96	0.51	0.96	1.96
MnO	0.013	0.013	0.009	0.005	0.006	0.006	0.005	0.01	0.01	0.01
CaO	0.73	0.5	1.96	0.47	0.16	0.21	0.2	0.16	0.60	1.96
Na_2O	2.75	3.75	4.92	8.88	2.05	3.15	3.91	2.05	4.20	8.88
K_2O	6.16	4.49	0.83	0.1	6.94	1.23	1.31	0.10	3.01	6.94
TiO_2	0.082	0.081	0.061	0.079	0.033	0.386	0.249	0.03	0.14	0.39
P_2O_5	0.05	0.05	0.04	0.03	0.05	0.06	0.05	0.03	0.05	0.06
*LOI	0.38	0.52	1.68	0.35	0.42	1.2	2.24	0.35	0.97	2.24
A/CNK	1.41	1.51	2.05	1.73	1.33	1.98	1.93	1.33	1.71	2.05

*LOI=Loss on ignition; A/CNK=$w(Al_2O_3)/w(CaO+Na_2O+K_2O)$; Min=Minimum value; Mean=Arithmetic average; Max=Maximum value

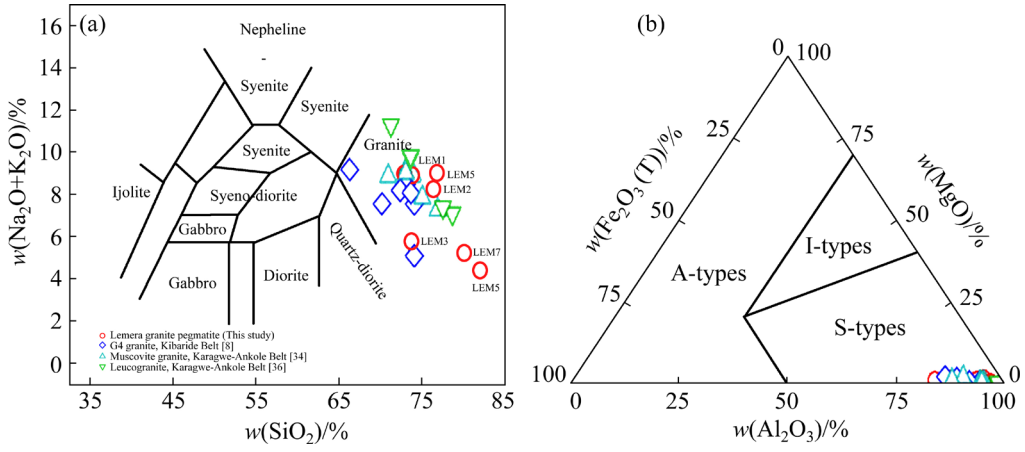

Fig. 4 (a) TAS diagram (total alkali−silica), displaying classification of magmatic rocks based on total alkali and silica abundance [37]; (b) Ternary diagram (after RAHMAN [38]) (The G_4 granite, muscovite granite and leucogranite samples were respectively collected from NAMBAJE et al [8], LEHMANN and LAVREAU [34], and POHL and GUNTHER [36])

pegmatites, and afterwards the iron oxides suddenly increased from the less evolved pegmatites to more evolved pegmatites (Fig. 5(a)). In contrast, TiO_2 content was low in the G_4 granites and increased readily from the less evolved pegmatites towards the most evolved pegmatites (Fig. 5(b)). Moreover, the K_2O content of both G_4 granites and Lemera pegmatites exhibited two different trends when plotted against SiO_2 content (Fig. 5(c)). Some samples showed higher K_2O content, and others had lower K_2O content in both G_4 granites and Lemera pegmatites. Besides, we noticed that most G_4 granites had a higher phosphorous content compared to the Lemera granite pegmatites (Fig. 5(d))

4.2 Bulk-rock trace and rare earth element compositions and geodynamic context

The statistics of some important whole rock trace elements of the Lemera granite pegmatites is listed in Table 2. The contents of tin (Sn) and zirconium (Zr) are found in the range of (1.00−138.00)×10^{-6} and (7.00−201.00)×10^{-6}, respectively. The compositional variation of some trace elements throughout the magmatic fluid evolution is presented in Fig. 6.

In Fig. 7, tectonic discrimination diagrams of the studied samples and those of the assumed parental granites are presented. All of the granite pegmatite samples, the leucogranite samples, and the majority of the muscovite granite samples fall into the field of a volcanic arc setting (Figs. 7(a, b, e)). Moreover, the Yb-normalized plot of Th and Ta indicates an active continental margin for all the studied pegmatite samples (Fig. 7(c)). It is worth noting that all the granite samples collected from literature, the Lemera granite pegmatites as well, fall in the range of peraluminous leucogranites associated with collisional zones, based on the w(Ta)/w(Zr) and w(Zr) discriminating parameters (Fig. 7(d)). In addition, one leucogranite sample

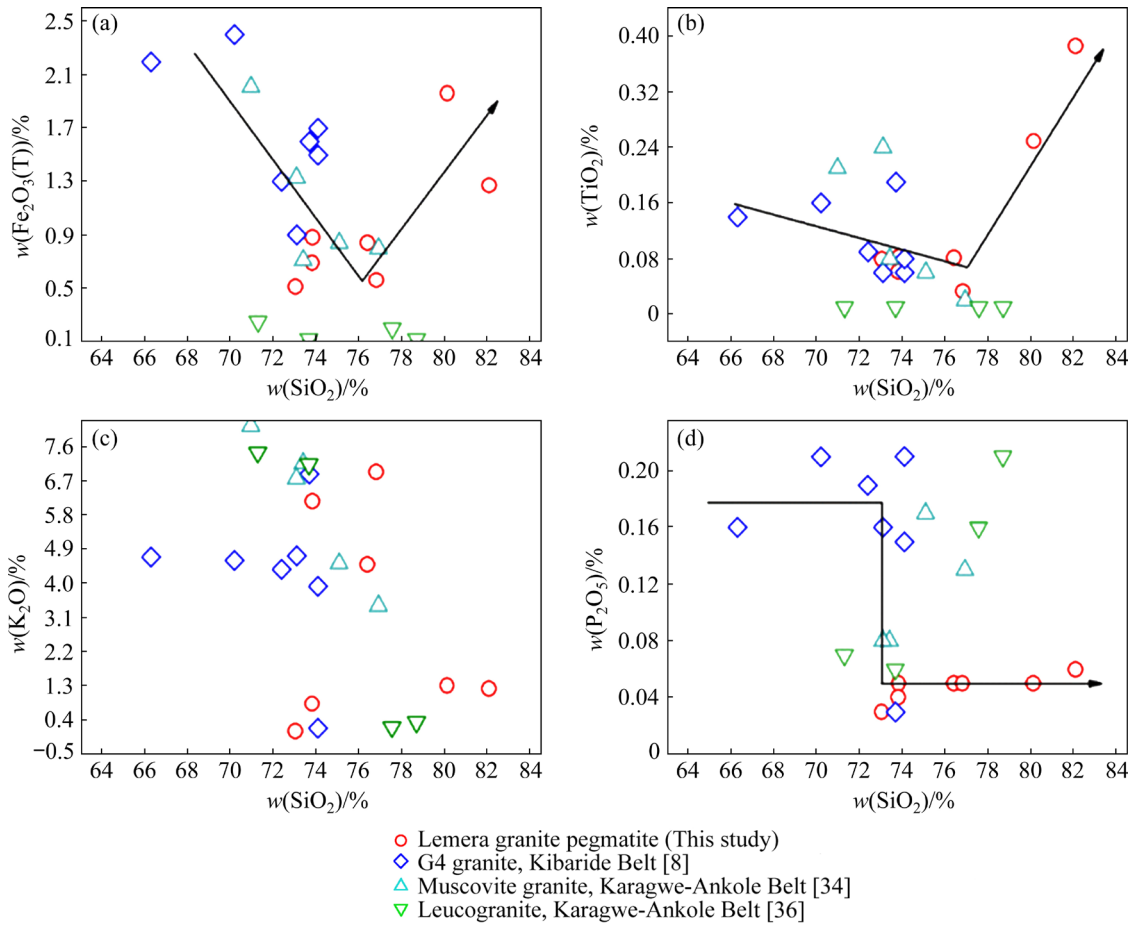

Fig. 5 Harker diagrams of Lemera granite pegmatites and G_4 granites (The arrow displays the major increase and/or decrease throughout the fractional crystallization from the G_4 Kibaran tin granites to the Lemera granite pegmatites. The G_4 granite, muscovite granite and leucogranite samples were respectively collected from NAMBAJE et al [8], LEHMANN and LAVREAU [34], and POHL and GÜNTHER [36])

Table 2 Statistics of bulk-rock compositions of rare earth (REE, Y and Sc), trace and other rare elements in Lemera granite pegmatites

Element type	Element	Number of sample	Content/10^{-6}			Detection method	Detection limit/10^{-6}
			Min	Mean	Max		
Rare earth elements, Y and Sc	La	7	4.10	11.51	26.30	ICP-MS	0.1
	Ce	7	9.60	22.93	55.20	ICP-MS	0.1
	Pr	7	1.20	2.49	5.88	ICP-MS	0.05
	Nd	7	4.60	9.24	21.90	ICP-MS	0.1
	Sm	7	1.10	2.06	4.20	ICP-MS	0.1
	Eu	7	0.19	0.62	0.93	ICP-MS	0.05
	Gd	7	0.70	1.76	3.40	ICP-MS	0.1
	Tb	7	0.20	0.27	0.50	ICP-MS	0.1
	Dy	7	0.50	1.31	2.60	ICP-MS	0.1
	Ho	7	0.10	0.25	0.50	ICP-MS	0.1
	Er	7	0.20	0.63	1.30	ICP-MS	0.1
	Tm	7	0.06	0.13	0.20	ICP-MS	0.05
	Yb	7	0.10	0.57	1.30	ICP-MS	0.1
	Lu	7	0.05	0.11	0.20	ICP-MS	0.01
	Y	7	2.00	6.33	13.00	XRF	1
	Sc	7	1.00	2.60	6.00	XRF	1
Trace and other rare elements	Be	7	1.00	1.40	2.00	XRF	1
	Ga	7	10.00	12.86	16.00	ICP-MS	1
	Rb	7	3.00	105.14	223.00	ICP-MS	2
	Cs	7	1.20	1.88	3.20	ICP-MS	0.5
	Sn	7	1.00	32.71	138.00	ICP-MS	1
	Sr	7	52.00	94.29	179.00	XRF	2
	Ba	7	9.00	277.00	411.00	XRF	2
	Zr	7	7.00	71.00	201.00	XRF	2
	Ta	7	0.20	0.33	0.60	ICP-MS	0.1
	Nb	7	1.00	3.33	8.00	ICP-MS	1
	b	7	0.50	2.28	5.50	ICP-MS	0.2
	W	7	8.00	9.00	10.00	ICP-MS	1
	Th	7	3.00	6.09	9.50	ICP-MS	0.1
	Bi	7	0.40	0.40	0.40	ICP-MS	0.4
	Tl	7	0.20	0.42	0.70	ICP-MS	0.1
	V	7	7.00	13.67	24.00	ICP-MS	5
	Ni	7	<20	<20	<20	ICP-MS	20
	Mo	7	<2	<2	<2	ICP-MS	2
	U	7	0.80	1.47	2.00	ICP-MS	0.1
	Cr	7	20.00	36.67	60.00	ICP-MS	20
	Co	7	2.00	2.00	2.00	ICP-MS	1
	Pb	7	21.00	93.00	307.00	ICP-MS	5

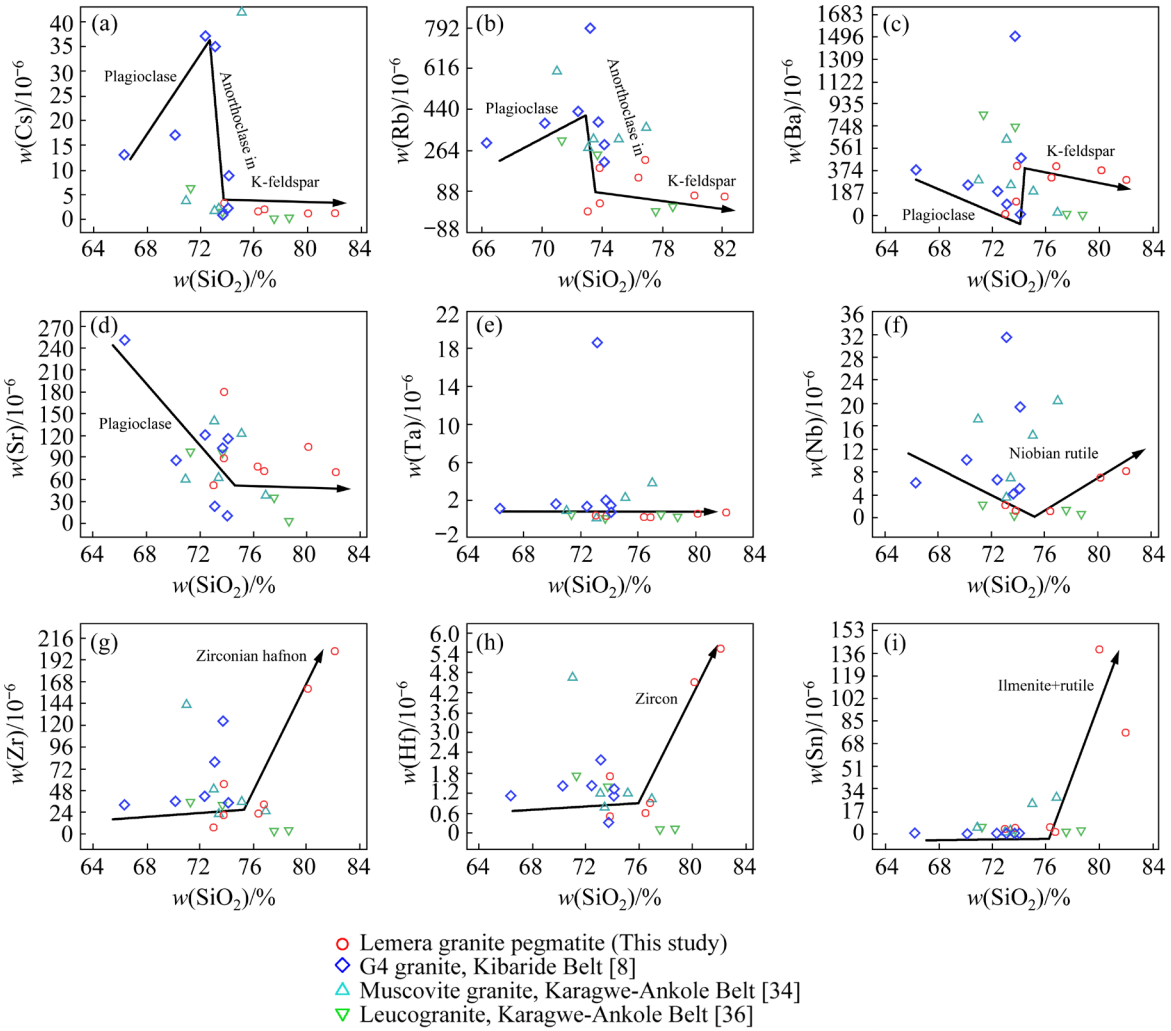

Fig. 6 Compositional variation of trace elements in Lemera granite pegmatites and G_4 granites, showing behavior (incompatible/compatible with given crystallizing mineral) of trace elements throughout magmatic fluid evolution (The G_4 granite, muscovite granite and leucogranite samples were respectively collected from NAMBAJE et al [8], LEHMANN and LAVREAU [34], and POHL and GUNTHER [36])

falls in the range of a late to post-collisional setting. In summary, our results suggest an active continental margin.

The Lemera granite pegmatites are slightly richer in LREE (light rare earth element) and depleted in HREE (heavy rare earth element) (Fig. 8). It is to be noticed that the majority of the Lemera granite pegmatite samples displayed a positive Eu anomaly (only a few samples presented a slight negative Eu anomaly), and this characteristic was also displayed by the leucogranite rocks of the KAB. Conversely, a majority of the G_4 granite samples showed a noticeable negative Eu anomaly, as did some samples of the muscovite granites of KAB, whilst some G_4 granite samples displayed no Eu anomaly.

5 Discussion

5.1 Petro-geochemistry of Lemera granite pegmatites

The Lemera granite pegmatites, G_4 granites, as well as muscovite granites and leucogranites suggest that they are all related to and are of S-type origin. This is sustained by the total alkali−silica diagram (TAS) and the ternary diagram of Fe_2O_3, MgO, and Al_2O_3 presented in Fig. 4. S-type granites are documented to be sourced from the melting of metamorphosed sedimentary rocks and/or sedimentary rocks or supracrustal rocks (Fig. 4(b)) [41]. As a result, pegmatitic rocks that fall within the range of S-type granites also reflect

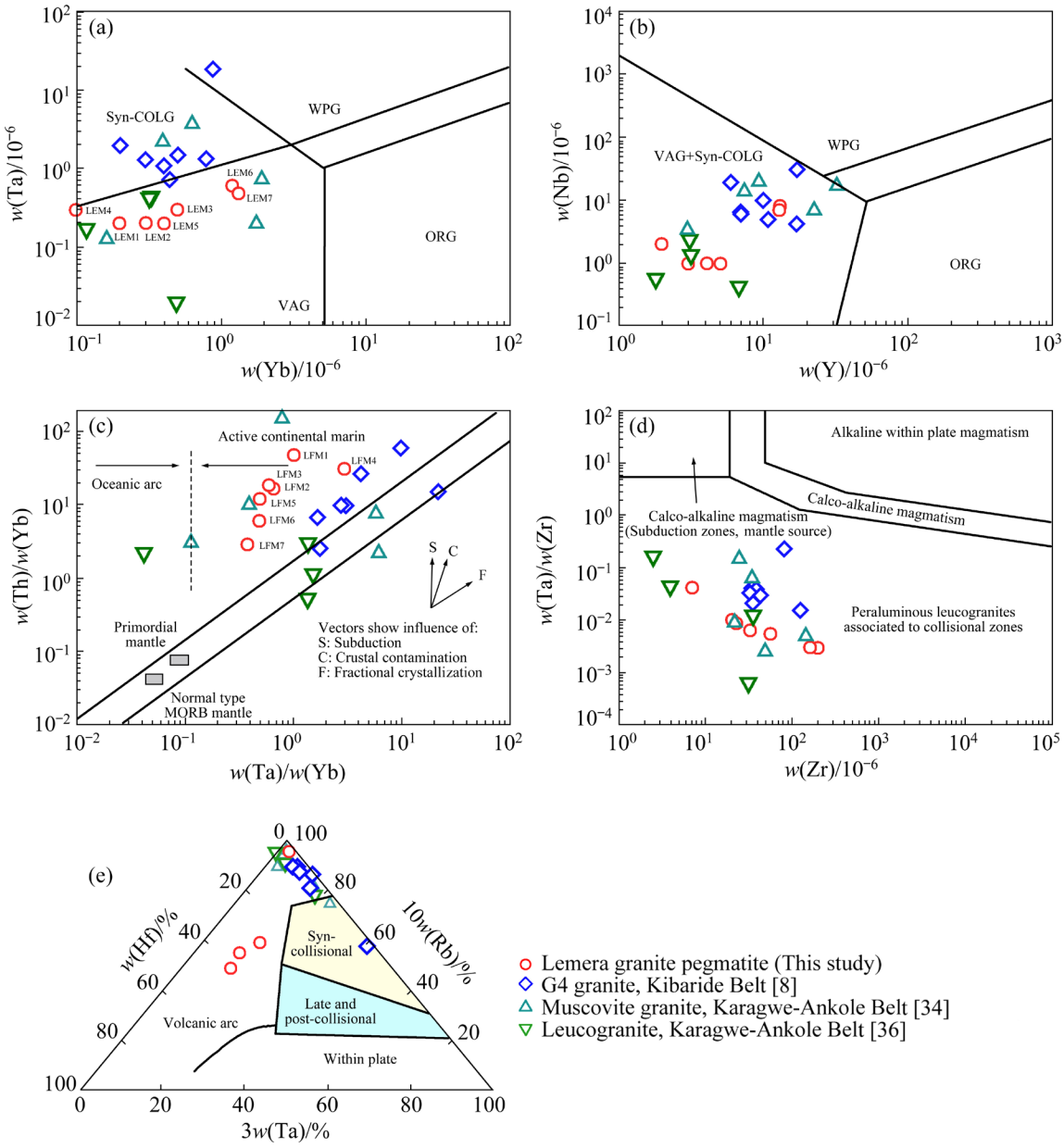

Fig. 7 Tectonic discrimination diagrams constraining geodynamic setting of G_4 granites and Lemera granite pegmatites (WPG: Within plate granite; ORG: Ocean ridge granite; COLG: Collisional granite; VAG: Volcanic arc granite [27,39,40]. The G_4 granite, muscovite granite and leucogranite samples were respectively collected from NAMBAJE et al [8], LEHMANN and LAVREAU [34], and POHL and GUNTHER [36])

the composition of the source material, which is derived from a metasedimentary source after having undergone a partial melting [42]. In the same way, the alumina saturation index (A/CNK) of the Lemera granite pegmatites ranges within 1.33−2.05, which confirms that these granitoids are mildly to strongly peraluminous and crystallized from a fertile granitic melt (A/CNK>1.0). Further, the mass fraction ratio of CaO to Na_2O (w(CaO)/w(Na_2O)) is within the ranges of 0.05−0.40 and 0.05−0.39, respectively, for the Lemera granite pegmatites and the G_4 granites. This ratio is in the same interval as the values reported by NAMBAJE et al [8] for the S-type granites of the KAB, which suggests that the melts could have derived from fluid-fluxed partial melting of metapelites. The mass fraction ratio of Rb to Sr (w(Rb)/w(Sr)) ranges within 0.06−3.14 and 1.18−34.35, while that of Rb to Ba (w(Rb)/w(Ba)) is in the interval of 0.19−0.54 and 0.26−30.71, for the Lemera granite pegmatites and the G_4 granites, respectively. These values suggest clay-rich source rocks [43].

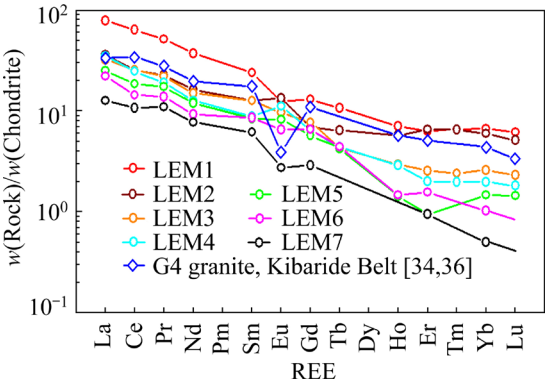

Fig. 8 Chondrite normalized REE patterns of regional G_4 granites of Kibaran Belt and Lemera granite pegmatites (The G_4 granite samples were collected from LEHMANN and LAVREAU [34], and POHL and GÜNTHER [36])

Moreover, the Harker diagram (Figs. 5(a) and (b)) implies that the onset of Fe−Ti oxide minerals such as rutile and ilmenite is similar to the behavior observed in Fig. 6(i), where Sn content increases significantly from the less evolved pegmatites to the more evolved pegmatites. This infers that the latter are likely to contain a sufficient quantity of cassiterite compared to the less evolved pegmatites of the Lemera area. However, in order to know which elements bear Sn element during the crystallization process, we have plotted the ratio of w(Ti)/w(Sn) against w(SiO_2) (Fig. 9(a)). The only Ti-bearing phase in reduced plutons is ilmenite, and the crystallization of the ilmenite is likely to have fostered the concentration of Sn as the magma was fractionating. Therefore, it is noteworthy to conclude that ilmenite and rutile accessory minerals are likely the main tin-bearing elements during the solidification of the Lemera granite pegmatites, since titanite does not crystallize in reduced granite pegmatites [44].

The behavior of phosphorous during the crystallization of magma depends on calcium activity [45], which somehow can be higher in peraluminous melts to form apatite or lower because the calcium that would crystallize the apatite minerals by consuming the phosphorous element was removed during the early crystallization of plagioclase [46]. Additionally, in more evolved pegmatites where the calcium is veritably lower, apatite cannot crystallize in such an environment. Thus, phosphorous and oxide elements might be incorporated into the alkali feldspars of the Lemera granite pegmatites (Figs. 5(c) and (d)) [47]. The onset of anorthoclase minerals and alkali feldspars in the Lemera granite pegmatites explains the negative and positive correlation observed in Figs. 6(a) and (b), respectively, since Rb and Cs elements are incompatible in plagioclase and compatible in the K-feldspars or either in the K-bearing minerals such as mica [22].

Further, Ba expressed a reverse correlation in Fig. 6(c) where the negative slope implies the crystallization of plagioclase because Ba is incompatible with plagioclase minerals. Specifically, the positive correlation displayed in intermediate samples might be due to the onset of calcic plagioclase because Ba seems to be incompatible with calcic plagioclase; finally, the decreasing slope means that Ba is incorporated into the alkali feldspars within the most evolved pegmatites [46]. Crystallization of feldspar minerals defines the decrease of Sr content as SiO_2 content increases from the G_4 granites towards the less evolved pegmatites. Afterwards, within the more evolved pegmatites, Sr content remains constant in the entire crystallization process (Fig. 6(d)), which infers that the more fractionated Lemera pegmatites contain high Rb content. This assumption is the characteristic of leucogranites, granite pegmatites and silicic rhyolites [21].

Next, the onset of either the niobium rutile minerals or the ilmenite minerals explains the inflection of Nb element (Fig. 6(f)) [48]. Zirconium and Hf may behave as identical twins during the magmatic crystallization process [49]. The w(Zr)/w(Hf) ratio readily remains intact through the entire fractionation trend (Fig. 9(b)), suggesting that Hf minerals do not crystallize during the magmatic differentiation process of pegmatites because of their low abundance in the continental crust [50,51]. Hence, these two elements (Zr and Hf) occurred together with zirconium into zircon accessory minerals. Consequently, the onset of zircon mineral crystallization defined the positive inflections displayed by Zr and Hf elements in Figs. 6(g) and (h).

In addition, it is noted that the retention of feldspars in the source rocks during the partial melting is plausible to explain the negative Eu anomaly and the positive Eu anomaly by the fractionation of quartz, plagioclase, and K-felspar during the pegmatite crystallization.

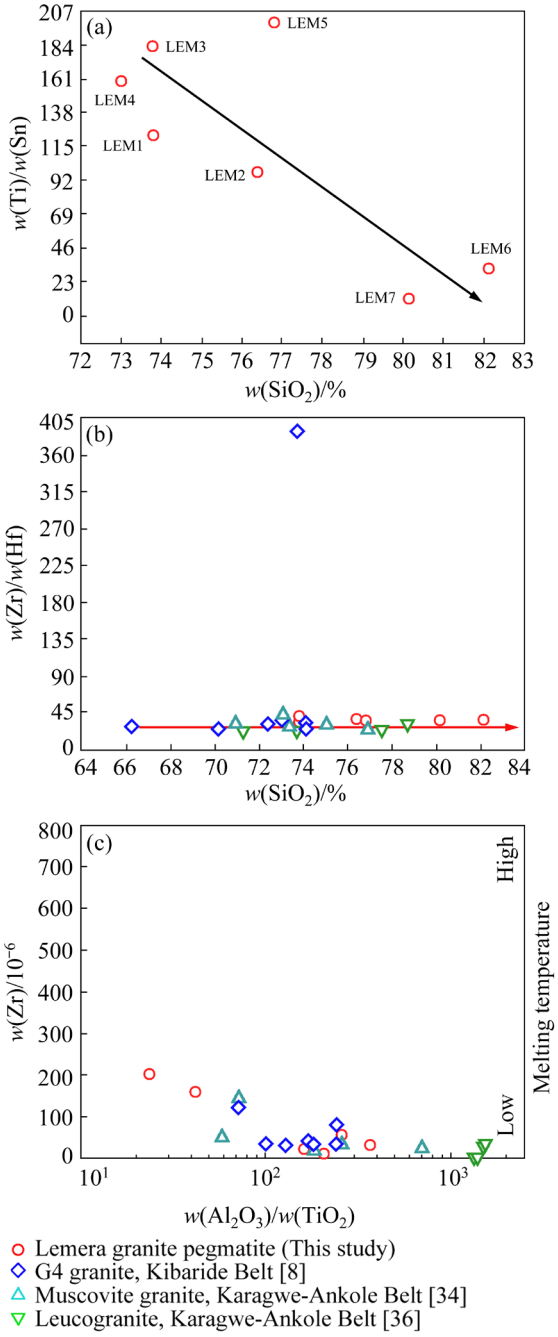

Fig. 9 (a) Variation diagram of w(Ti)/w(Sn) ratio versus w(SiO_2) (The linear curve of the samples from Lemera granite pegmatites shows a negative linear correlation, with w(Ti)/w(Sn) values decreasing from the less evolved pegmatites to the more evolved pegmatites); (b) Diagram of w(Zr)/w(Hf) ratio versus w(SiO_2), inferring behavior of Zr and Hf during Lemera granite pegmatites crystallization; (c) Diagram of w(Zr) versus w(Al_2O_3)/w(TiO_2), indicative of the relative variation trend in temperature of melting [50] (The G_4 granite, muscovite granite and leucogranite samples were respectively collected from NAMBAJE et al [8], LEHMANN and LAVREAU [34], and POHL and GÜNTHER [36])

5.2 Tectono-magmatism context of Lemera granite pegmatites

The tectonic diagrams of the studied samples suggested an active continental margin as the prominent setting (Fig. 7). This has been supported by the most recent research conducted in the KAB [8]. The regional tectono-magmatic models proposed by recent research and sustained by geochronological, structural, and petrological data, suggest the emplacement of the G_4 granites, muscovite granites, and leucogranites, as well as the Numbi pegmatites and the Gatumba pegmatites, from (1011±18) Ma to (976±11) Ma, in a late to post-collisional setting, and are associated with the D2 orogenic event (1078 Ma). The latter consisted of a continental collision during the final stage of Rodinia assembly [8,27]. Moreover, NAMBAJE et al [20] reported shearing and reverse faulting structures that are associated with the main episode of Sn mineralization occurring from 1090 to 960 Ma in the KAB. These compressional-deformational structures support the above-mentioned collisional setting. Because the forementioned granitoids have shown strong chemical composition and spatiotemporal relationships with the Lemera granite pegmatites that are studied in this work, we infer that the pegmatites were emplaced in a late to post collisional setting (Figs. 10(a, b)). The volcanic arc setting, suggested by some diagrams in Fig. 8, for all of the analyzed granite pegmatite and leucogranite samples, and the majority of the muscovite granite samples, could be explained by the fact that late to post collisional magmatism may involve materials from diverse sources, including older granites (e.g., S-type granite emplaced in a volcanic arc setting). This possibility needs to be further studied for evidence.

5.3 Genesis of Lemera granite pegmatites and its related tin ore deposits

The evidence of chemical and spatiotemporal relationships between the Lemera granite pegmatites and the G_4 granites confirms that the likely mechanism of emplacement of the studied pegmatites is fractional crystallization of a granitic melt. Here, the fertility of the granitic melt, the degree of fractional crystallization, as well as the enrichment of rare metals, especially Sn, are discussed. The fertility of the parental granitic melt

has been established earlier in this study, based on the alumina saturation index A/CNK and the ternary diagram of Fe_2O_3 (T), MgO, and Al_2O_3. Therefore, this section focuses on rare element proxies.

Tables 3 [52,53] and 4 display the ranges of rare elements in the upper-continental crust as well as those of typical pegmatitic fertile granite (bulk rock), which helped to further categorize the fertility of the granitic melt that evolved towards the Lemera granite pegmatites and to assess the enrichment level of rare metals. Moreover, the mass fraction ratios of w(K)/w(Rb), w(K)/w(Cs), and w(Nb)/w(Ta) are widely used as fertility indicators

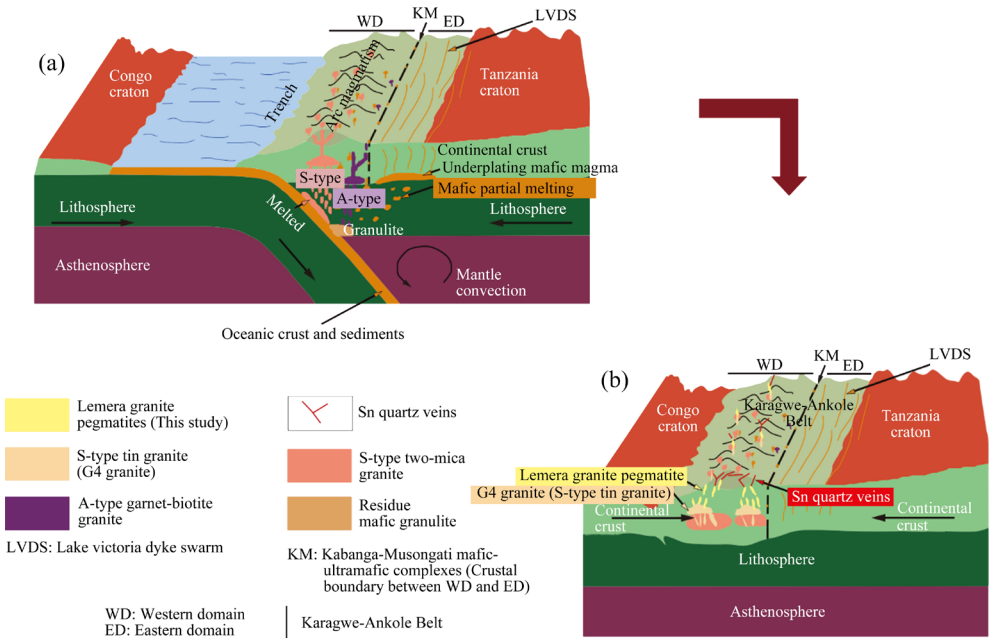

Fig. 10 Tectono-magmatism model of granitoids of Karagwe-Ankole Belt, including Lemera granite pegmatites (after NAMBAJE et al [8]): (a) D1 orogenic event, emplacement of S-type two-mica granite and contemporaneous A-type garnet-biotite granite ((1380−1360) Ma): Accretion during early stage or Rodinia Assembly; (b) D2 orogenic event (~1078 Ma), emplacement of late to post-collisional S-type tin granites ((1011−976) Ma) and probably the Lemera pegmatite analyzed in this study: Continental collision during final stage of Rodinia Assembly

Table 3 Bulk-rock compositions of rare elements in crustal rocks and pegmatites [52,53]

Rare element	Average content of upper continental crust/10^{-6}	Internal pegmatitic granite						Separation rapids pluton	
		Fine-grained leucogranite		Pegmatitic leucogranite		Sodic aplite			
		Mean/10^{-6}	Range/10^{-6}	Mean/10^{-6}	Range/10^{-6}	Mean/10^{-6}	Range/10^{-6}	Mean/10^{-6}	Range/10^{-6}
Be	3	4	0.5−61	27	0.5−604	6	1−34	6.2	3.3−25
Cs	3.7	8	0.5−39	14	0.5−51	16	0.2−67	48	11.8−172
Ga	17	38	10−81	20	10−90	9	45−73	36	21−94
Li	20	81	1−1400	51.7	6−288	82	7−324	235	71−1629
Nb	25	24	1−81	18	1−135	−	45−138	66	32−120
Rb	112	305	33−1050	473	32−5780	169	9−559	890	341−1240
Sn	5.5	9	1−44	19	1−112	13	2−25	62	10−652
Ta	2.2	4.5	2−8.5	2.7	0.5−8	−	3−435	19	6.6−29.7
w(K)/w(Cs)	7630	11000	794−78400	7880	246−38500	3020	166−14900	852	35−1526
w(K)/w(Rb)	252	159	42−418	165	13−576	85	24−332	34	0.5−51
w(Nb)/w(Ta)	11.4	5	0.1−11.9	1.71	0.1−7.17	−	0.32−0.62	4.5	0.9−6.9

Table 4 Bulk-rock compositions of rare elements in Lemera granite pegmatites

Rare element	Pegmatitic leucogranite content range/10^{-6}	Content of analyzed samples/10^{-6}									
		LEM1	LEM2	LEM3	LEM4	LEM5	LEM6	LEM7	Min	Mean	Max
Be	1−604	−	1	2	1	−	1	2	1.00	1.40	2.00
Ga	19−90	13	13	15	16	10	11	12	10.00	12.86	16.00
Rb	32−5775	188	145	37	3	223	68	72	3.00	105.14	223.00
Cs	0.5−51	2.2	1.6	3.2	−	1.9	1.2	1.2	1.20	1.88	3.20
Y	3−102	2.3	4	5	2	5	13	13	2.00	6.33	13.00
Sn	1−112	4	5	2	3	1	76	138	1.00	32.71	138.00
Ti	100−4300	991.6	485.6	365.6	473.6	197.8	2314	1492	197.80	902.89	2314.00
Sr	1−495	89	77	179	52	91	69	103	52.00	94.29	179.00
Ba	6−900	411	318	115	9	410	299	377	9.00	277.00	411.00
Zr	1−77	20	22	55	7	32	201	160	7.00	71.00	201.00
Ta	0.5−8	0.2	0.2	0.3	0.3	0.2	0.6	0.5	0.20	0.33	0.60
Nb	1−135	1	1	1	2	−	8	7	1.00	3.33	8.00

of the parental granite [53]. The average values of these elements in a fertile granite are supposed to be lower than the average values of the upper-continental crust (Table 3). The Lemera granite pegmatites have shown lower values than the upper-continental crust for all the above-mentioned ratios, except w(K)/w(Cs), which show a slightly higher average value. Further, the average mass fraction ratio of Nb to Ta (w(Nb)/w(Ta)) of the analyzed samples is inferior to height, which confirms the fertility of the granitic magma that evolved towards the studied pegmatites [53]. Furthermore, the ranges of selected rare elements of the studied Lemera granite that are displayed in Table 4 verify the inference stated above regarding the fertility of the granitic melt. Indeed, the ranges of all the selected rare elements are in the respective intervals of pegmatitic leucogranites. It is worth noting that Sn and Zr show some values beyond the interval. This is also supported by the rare element mass fraction ratios, presented in Table 5.

The rare elements and their related parameters presented in Tables 4 and 5 are also widely used to evaluate the degree of fractional crystallization [52,54,55]. Sr, Ti, Ta, Ba, Sn, Ga, Nb, Y, Li, Cs, Rb, and Be contents generally increase with the evolution of fractional crystallization, while w(Zr), w(K)/w(Cs), w(K)/w(Rb), w(Nb)/w(Ta), w(Ba)/w(Rb), w(Zr)/w(Hf), w(Zr)/w(Sn), and w(Zr)/w(Y) generally decrease with the evolution of fractionation [52,55]. During the fractionation of granitic melts, the first products that are yielded are barren granite pegmatites, followed by mineralized granite pegmatites owing to the enrichment of incompatible elements and volatile components into the residual melt during the evolution of fractionation processes [46,54,56]. CERNY and ERCIT [57] proposed a degree of fractionation of ≥99% of the parental melt for the most fractionated units of up to $>100\times10^{-6}$ Ta (the less fractionated unit of which contains $\leq1\times10^{-6}$ Ta). In the Karagwe-Ankole Belt, the Gatumba pegmatites are the most documented and well-studied pegmatites. Previous studies have divided the latter into 4 zones regarding the degree of fractional crystallization, which include Zone-1 (biotite zone: 0−69% of crystallization), Zone-2 (two-mica zone: 69%−92% of crystallization), Zone-3 (muscovite zone: 92%−98% of crystallization), and Zone-4 (mineralized zone: >98% of crystallization). Zone-4 is mainly enriched in Nb, Ta, and Sn [28]. Based on the content range of Ta of the Lemera granite pegmatite samples analyzed in this study, which is from 0.20×10^{-6} to 0.60×10^{-6}, we infer that they belong to the less fractionated pegmatites of the region. This is further supported by the ranges of most of the mass fraction ratios presented in Table 5, which are at least close to or beyond the upper limits of typical fertile granites (e.g., w(Nb)/w(Ta), w(K)/w(Cs), and w(K)/w(Rb)). The Numbi pegmatites (pegmatite veins), which are located in the Congolese part of the Karagwe-Ankole Belt, in

Table 5 Ranges of fertile granite and fractionation indicators of Lemera granite pegmatites [52,55]

Ratio	Fertile granite content range/10^{-6}	Content of analyzed samples/10^{-6}							Min	Mean	Max
		LEM1	LEM2	LEM3	LEM4	LEM5	LEM6	LEM7			
w(K)/w(Cs)	1600−15400	23245	23257	2153	8509	9.063	1121	−	9.06	9716	23257
w(K)/w(Rb)	42−270	272	252	186	151	208	150	−	150.00	203.17	272.00
w(K)/w(Ba)	48−18250	124	117	59.9	92.2	140	34.15	−	34.15	94.54	140.00
w(Nb)/w(Ta)	0.1−7.17	5	5	3.33	6.66	−	13	14	3.33	7.83	14.00
w(Rb)/w(Sr)	1.6−185	2.7	186	0.2	0	3.1	0.9	0.7	0	27.66	186.00
w(Zr)/w(Hf)	14−64	40	36	32	−	35	36	35	32.00	35.67	40.00

the same administrative province as the Lemera study area (Lat. 1.75°−2.00° and Long. 28.75°−29.00°), show values that suggest a more advanced degree of fractionation w(Nb)/w(Ta)=(0.27−115)×10^{-6} (0.77×10^{-6} average), w(K)/w(Rb)=(14.61−67.00)×10^{-6}, w(Ta)=(27.5−370.9)×10^{-6}, w(Sn)=(56−2451)×10^{-6}, and w(Nb)=(53.7−139.2)×10^{-6} [57]. The relationship between the Numbi pegmatites and the Lemera granite pegmatites is worth further study.

In addition, the samples collected along the Kakwende River (LEM1, LEM2, LEM3, LEM4, and LEM5), which are considered the less evolved Lemera granite pegmatites based on the Harker diagram (showing the evolution of Fe_2O_3, TiO_2, K_2O, and P_2O_5 against SiO_2) and the compositional variation of trace elements presented in Figs. 5 and 6, respectively, exhibit significantly lower contents of Sn ((1−5)×10^{-6}), and Zr ((7−55)×10^{-6}) (Table 4) compared to the more evolved pegmatites of the Lemera study area, which show the enrichment in Sn and Zr, compared to the upper-continental average values (Table 3), and the typical fertile pegmatitic leucogranite (Table 4) (w(Sn)=(76−138)×10^{-6} and w(Zr)=(160−201)×10^{-6}). The enrichment of Sn, Hf, and Zr in the more evolved pegmatites could be attributed to fractional crystallization. This is corroborated by the evolutionary trend of Ta content, which increases, and the evolutionary trends of w(K)/w(Cs) and w(K)/w(Rb) that decrease from the Kakwende River samples towards the Kigunga sector samples. However, the mass fraction ratio of Nb to Ta (w(Nb)/w(Ta)) that is supposed to decrease with fractional crystallization, presents an increasing trend, which needs to be further studied using specific mineral chemistry.

Relying on the pegmatite classification scheme proposed by CERNY and ERCIT [57] using petrogenetic and geochemical characteristics and updated by BRADLEY et al [58], the Lemera granite pegmatites belong to the lithium−cesium−tantalum (LCT) family and are linked to the rare element class pegmatites. The evidence discussed above, including the inferred characteristics of the granitic melt from which they crystallized (e.g., peraluminous, S-type granitic melt, and fertile granitic melt), supports this. The diagram of w(Al_2O_3)/ w(TiO_2) versus w(Zr) suggests a lower melting temperature, as well (Fig. 9(c)). It can be assumed that their crystallization occurred at a low temperature in a relatively short time [58]. This is also a characteristic of typical LCT pegmatites. However, the low abundances of Cs, Ta, and Be suggest that they belong to the less evolved zone of the LCT pegmatitic field.

Based on the Sn and Zr enrichments throughout the assumed fractional crystallization, among the samples collected along the Kigunga sector, which are significantly in contrast with the Kakwende River samples, we conclude that the Lemera region has two geochemical evolutionary signatures (Fig. 11), which are: (1) the less fractionated pegmatitic signature that typifies the samples collected along the Kakwende River, which do not record any mineralization; (2) the more fractionated pegmatitic signature, which characterizes the samples collected near the Kigunga sector where mineralization of Sn and Zr is noticed.

It is worth noting that the terms "less fractionated" and "more fractionated" are used in order to compare the Sn mineralized Lemera granite pegmatites to the barren Lemera granite pegmatites. Furthermore, the above-discussed evidence shows

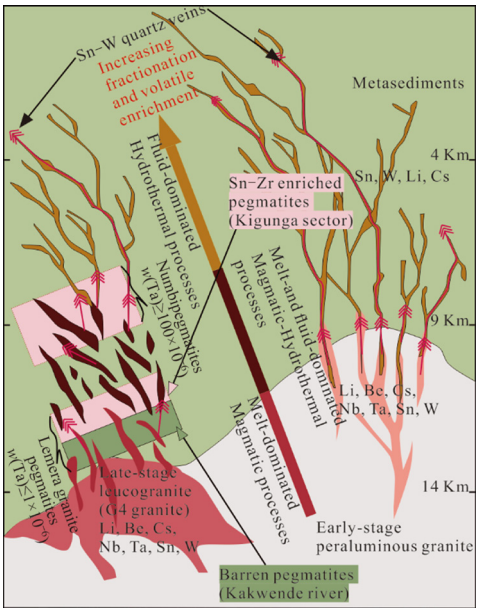

Fig. 11 Metallogenic model for development of Nb−Ta−Sn pegmatite-type and Sn−W quartz vein-type deposits in Lemera area (after HULSBOSCH [59]) (Lithium enrichment was omitted from the pegmatite zone, because it was not studied in this work)

that the Sn mineralization, which is noticed in samples collected near the Kigunga sector, is likely to have occurred during the second generation and the peak of Sn mineralization in the KAB (1040−960 Ma) [20]. Moreover, accessory minerals such as ilmenite and rutile are likely the main tin-bearing minerals during the solidification of the Lemera granite pegmatites.

5.4 Comparative analysis of lemera granite pegmatites, Gatumba pegmatites and Numbi pegmatites

A brief discussion regarding the fractionation degree of the Lemera granite pegmatites compared to the Gatumba pegmatites and the Numbi pegmatites is presented. Thanks to its remarkable well-developed regional zoning, the Gatumba pegmatite field is a first-class area for the investigation of granite−pegmatite differentiation processes [17]. The four zones that make up the field were presented in the previous section. Here, selected indicators of fractionation listed in Tables 4 and 5 are used for the comparison of the above-cited pegmatites of the Karagwe-Ankole Belt. All the pegmatites forementioned are likely products of the fractional crystallization of a peraluminous S-type granitic melt (G_4 granite), which are similar to other granitic rocks in South China [60−63]. They are connected tectonically and temporally, based on the results discussed in this study and some others in previous research [18,27].

As stated in the previous section, it is widely accepted and proven that the ratios of w(K)/w(Rb) and w(K)/w(Cs) decrease throughout fractional crystallization because the residual melt becomes continually enriched in Rb and Cs and depleted in K during the magmatic crystallization of pegmatites [46]. The ratio of w(K)/w(Rb) is plotted against w(Cs) and w(Rb), respectively, in Figs. 12(a) and (c).

These diagrams place the Lemera granite in the location occupied by the pegmatites of Zone-1 to Zone-3 in the Gatumba pegmatite field [17], while the Numbi pegmatites fall in the range of the Gatumba mineralized pegmatite (Zone-4). This supports the inference of the previous section of lower fractionation degree for the Lemera granite pegmatites. Moreover, the diagrams of the ratios of w(Zr)/w(Hf) and w(Nb)/w(Ta) against w(Zr) and w(Ta), respectively, confirm as well that the Lemera granite pegmatites belong to a less evolved zone of the pegmatite field, while the Numbi pegmatites are highly fractionated (Figs. 12(b) and (d)). Furthermore, from the comparison discussed, we infer that the Lemera granite pegmatites and the Numbi pegmatites are members of pegmatite fields, and further studies are suggested in order to understand the extension of those fields or the possible connection of both pegmatites, in case they constitute the same large field.

In addition, this study is limited to whole rock geochemical analyses, thus further studies on mineral chemistry are required in order to elucidate the mineralization of Sn in the pegmatites that show characteristics of the less fractionated pegmatitic zone, based on the scale proposed by CERNY and ERCIT [57] on the one hand, and on the other hand, based on the values of the following values w(Nb)/w(Ta), w(Zr)/w(Hf), w(K)/w(Rb), w(K)/w(Cs), w(Ta), w(Nb), and w(Cs), compared to those of a well-studied and developed pegmatite field (the Gatumba pegmatites), as well as the Numbi pegmatites, both located in the of Karagwe-Ankole Belt.

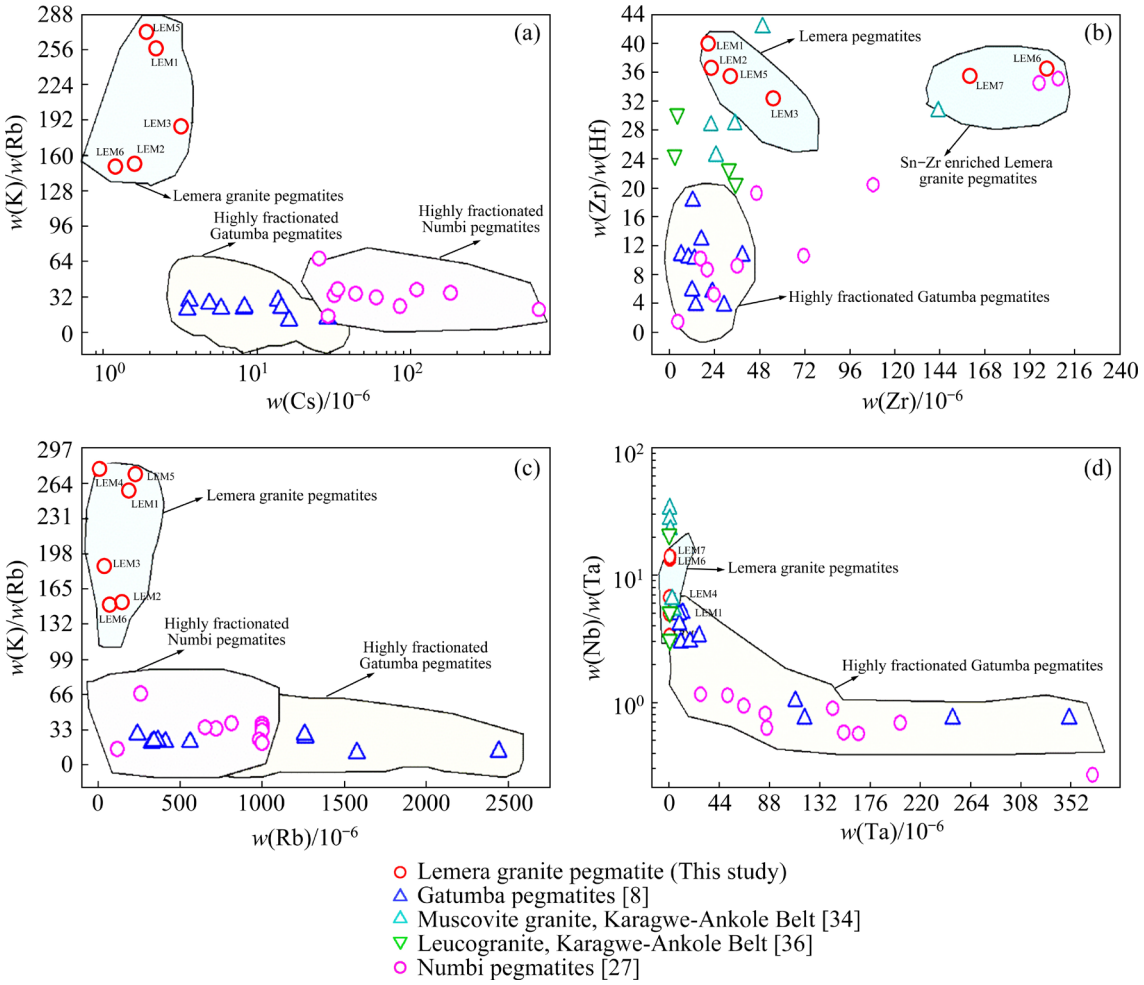

Fig. 12 Diagrams of w(K)/w(Rb) versus w(Cs) (a), w(Zr)/w(Hf) versus w(Zr) (b), w(K)/w(Rb) versus w(Rb) (c) and w(Nb)/w(Ta) versus w(Ta) (d) (The data of the Gatumba pegmatites, Numbi pegmatites, muscovite granites and leucogranite pegmatites of the KAB are collected from NAMBAJE et al [8], OYEDIRAN et al [27], LEHMANN and LAVREAU [34], POHL and GÜNTHER [36], respectively)

6 Conclusions

(1) The analyzed Lemera granite pegmatites samples show a relative abundance of Al_2O_3 over Fe_2O_3 (T) and MgO (12.95 wt.%, 0.96 wt.%, and 0.16 wt.%, respectively). The SiO_2 content ranges from 73.04 wt.% to 82.10 wt.%, while the total content of Na_2O and K_2O ranges from 4.38 wt.% to 8.99 wt.%. The alumina saturation index (A/CNK) ranges from 1.33 to 2.05. The abundances of some important rare metals, as well as some related key parameters, are determined.

(2) The Lemera granite pegmatites crystallized from a fertile, peraluminous, and S-type granitic magma through a fractional crystallization process. Furthermore, the spatiotemporal and chemical relationships with the G_4 granites (assumed parental granite) were established, while their emplacement has been constrained in a late to post-collisional setting, probably related to the documented magmatism occurring at 1011−976 Ma, based on the chemical composition of rare element proxies.

(3) The Sn and Zr mineralization led to a zonation of the Lemera granite pegmatite, which has been sustained by the trend of some fractional crystallization proxies. This local fractional evolution distinguishes the less fractionated pegmatitic signature that typifies the samples collected along the Kakwende River. Ilmenite and rutile are likely to be the main tin-bearing minerals during the solidification of the Lemera granite pegmatites.

Acknowledgments

This study was supported by the National Natural Science Foundation of China (No. 92162103), the Natural Science Foundation of Hunan Province, China (No. 2022JJ30699), the Science and Technology Innovation Program of Hunan Province, China (No. 2021RC4055), and the Open Research Project from the State Key Laboratory of Geological Processes and Mineral Resources, China University of Geosciences (No. GPMR202112).

References

[1] HU Xiao-jun, LI Huan. Research progress and prospect of granitic pegmatite-type lithium deposits [J]. The Chinese Journal of Nonferrous Metals, 2021, 31(11): 3468−3488 (in Chinese)

[2] DILL H G. Pegmatites and aplites: Their genetic and applied ore geology [J]. Ore Geology Reviews, 2015, 69: 417−561.

[3] FERNANDEZ-ALONSO M, CUTTEN H, DE WAELE B, TACK L, TAHON A, BAUDET D, BARRITT S D. The Mesoproterozoic Karagwe-Ankole Belt (formerly the NE Kibara Belt): The result of prolonged extensional intracratonic basin development punctuated by two short-lived far-field compressional events [J]. Precambrian Research, 2012, 216/217/218/219: 63−86.

[4] TACK L, WINGATE M T D, DE WAELE B, MEERT J, BELOUSOVA E, GRIFFIN B, TAHON A, FERNANDEZ-ALONSO M. The 1375 Ma "Kibaran event" in Central Africa: Prominent emplacement of bimodal magmatism under extensional regime [J]. Precambrian Research, 2010, 180(1/2): 63−84.

[5] DEBRUYNE D, HULSBOSCH N, VAN WILDERODE J, BALCAEN L, VANHAECKE F, MUCHEZ P. Regional geodynamic context for the Mesoproterozoic Kibara Belt (KIB) and the Karagwe-Ankole Belt: Evidence from geochemistry and isotopes in the KIB [J]. Precambrian Research, 2015, 264: 82−97.

[6] KAMPUNZU A B, RUMVEGERI B T, KAPENDA D, LUBALA R T, CARON J P H. Kibarides in central and east africa: A collision chain [J]. UNESCO, Geology for Development Newsletter, 1986, 5: 125−137.

[7] RUMVEGERI B T. Tectonic significance of Kibaran structures in central and eastern Africa [J]. Journal of African Earth Sciences, 1991, 13: 267−276.

[8] NAMBAJE C, SATISH-KUMAR M, WILLIAMS I S, TAKAHASHI T, SAJEEV K. Granitic rocks from Rwanda: Vital clues to the tectonic evolution of the Karagwe-Ankole Belt [J]. Lithos, 2021, 404/405: 106490.

[9] KLERKX J, LIÉGEOIS J P, LAVREAU J, CLAESSENS W. Crustal evolution of the northern Kibaran Belt, eastern and central Africa [M]//Proterozic Lithospheric Evolution. Washington D. C.: American Geophysical Union, 1987: 217−233.

[10] CAHEN L, SNELLING N, DELHAL J, VAIL J, BONHOMME M, LEDENT D. The geochronology and evolution of African [M]. Oxford: Clarendon, 1984.

[11] FERNANDEZ-ALONSO M, LAVREAU J, KLERKX J. Geochemistry and geochronology of the Kibaran granites in Burundi, central Africa: Implications for the Kibaran orogeny [J]. Chemical Geology, 1986, 57(1/2): 217−234.

[12] TACK L, LIÉGEOIS J P, DEBLOND A, DUCHESNE J C. Kibaran A-type granitoids and mafic rocks generated by two mantle sources in a late orogenic setting (Burundi) [J]. Precambrian Research, 1994, 68(3/4): 323−356.

[13] DELVAUX D, MULUMBA J L, SEBAGENZI M N S, BONDO S F, KERVYN F, HAVENITH H B. Seismic hazard assessment of the Kivu rift segment based on a new seismotectonic zonation model (western branch, East African Rift system) [J]. Journal of African Earth Sciences, 2017, 134: 831−855.

[14] KUSKY T M, ABDELSALAM M, TUCKER R D, STERN R J. Evolution of the East African and related orogens, and the assembly of Gondwana [J]. Precambrian Research, 2003, 123(2/3/4): 81−85.

[15] DEWAELE S, CLERCQ F, HULSBOSCH N, PIESSENS K, BOYCE A, BURGESS R, MUCHEZ P. Genesis of the vein-type tungsten mineralization at Nyakabingo (Rwanda) in the Karagwe–Ankole Belt, central Africa [J]. Mineralium Deposita, 2016, 51(2): 283−307.

[16] HULSBOSCH N, HERTOGEN J, DEWAELE S, ANDRÉ L, MUCHEZ P. Petrographic and mineralogical characterisation of fractionated pegmatites culminating in the Nb−Ta−Sn pegmatites of the Gatumba area (western Rwanda) [J]. Geologica Belgica, 2013, 16: 105−117.

[17] WU Jing-hua, LI Huan, MATHUR R, BOUVIER A, POWELL W, YONEZU K, ZHU Da-peng. Compositional variation and Sn isotope fractionation of cassiterite during magmatic-hydrothermal processes [J]. Earth and Planetary Science Letters, 2023, 613: 118186.

[18] LEHMANN B, HALDER S, RUZINDANA MUNANA J, PAIX NGIZIMANA J, BIRYABAREMA M. The geochemical signature of rare-metal pegmatites in Central Africa: Magmatic rocks in the Gatumba tin−tantalum mining district, Rwanda [J]. Journal of Geochemical Exploration, 2014, 144: 528−538.

[19] POHL W L, BIRYABAREMA M, LEHMANN B. Early Neoproterozoic rare metal (Sn, Ta, W) and gold metallogeny of the Central Africa Region: A review [J]. Applied Earth Science, 2013, 122(2): 66−82.

[20] NAMBAJE C, WILLIAMS I S, SAJEEV K. SHRIMP U−Pb dating of cassiterite: Insights into the timing of Rwandan tin mineralisation and associated tectonic processes [J]. Ore Geology Reviews, 2021, 135: 104185.

[21] BALLOUARD C, ELBURG M A, TAPPE S, REINKE C, UECKERMANN H, DOGGART S. Magmatic-hydrothermal evolution of rare metal pegmatites from the Mesoproterozoic Orange River pegmatite Belt (Namaqualand, South Africa) [J]. Ore Geology Reviews, 2020, 116: 103252.

[22] ZHENG Fan-bo, WANG Guo-guang, NI Pei. Research progress on the fluid metallogenic mechanism of granitic pegmatite-type rare metal deposits [J]. Journal of Geomechanics, 2021, 27(4): 596−613.

[23] DAELE J V, HULSBOSCH N, DEWAELE S, BOIRON M C, PIESSENS K, BOYCE A, MUCHEZ P. Mixing of magmatic-hydrothermal and metamorphic fluids and the origin of peribatholitic Sn vein-type deposits in Rwanda [J]. Ore Geology Reviews, 2018, 101: 481−501.

[24] NAMBAJE C, EGGINS S M, YAXLEY G M, SAJEEV K. Micro-characterisation of cassiterite by geology, texture and zonation: A case study of the Karagwe Ankole Belt, Rwanda [J]. Ore Geology Reviews, 2020, 124: 103609.

[25] DEWAELE S, CLERCQ F D, MUCHEZ P, SCHNEIDER J, BURGESS R, BOYCE A, ALONSO M. Geology of the cassiterite mineralisation in the Rutongo area, Rwanda (central Africa): Current state of knowledge [J]. Geologica Belgica, 2010, 13: 91−111.

[26] HULSBOSCH N, van DAELE J, REINDERS N, DEWAELE S, JACQUES D, MUCHEZ P. Structural control on the emplacement of contemporaneous Sn−Ta−Nb mineralized LCT pegmatites and Sn bearing quartz veins: Insights from the Musha and Ntunga deposits of the Karagwe-Ankole Belt, Rwanda [J]. Journal of African Earth Sciences, 2017, 134: 24−32.

[27] OYEDIRAN I A, NZOLANG C, MUPENGE M P, IDAKWO S O. Structural control and Sn−Ta−Nb mineralization potential of pegmatitic bodies in Numbi, South Kivu Eastern D. R Congo [J]. Lithos, 2020, 368/369: 105601.

[28] HULSBOSCH N, HERTOGEN J, DEWAELE S, ANDRÉ L, MUCHEZ P. Alkali metal and rare earth element evolution of rock-forming minerals from the Gatumba area pegmatites (Rwanda): Quantitative assessment of crystal-melt fractionation in the regional zonation of pegmatite groups [J]. Geochimica et Cosmochimica Acta, 2014, 132: 349−374.

[29] de DIEU NDIKUMANA J, MUPENGE P M, NAMBAJE C, RAOELISON I L, BOLARINWA A T, ADEYEMI G O. Structural control on the Sn−Ta−Nb mineralisation and geochemistry of the pegmatites of Gitarama and Gatumba areas (Rwanda), Karagwe-Ankole Belt [J]. Arabian Journal of Geosciences, 2021, 14(23): 1−19.

[30] NAMBAJE C, WILLIAMS I S, SATISH-KUMAR M, SAJEEV K. Direct evidence for Archean crust in the western domain of the Karagwe Ankole Belt, Rwanda: Implications for Neoarchean to Paleoproterozoic crustal evolution [J]. Precambrian Research, 2020, 350: 105851.

[31] KOKONYANGI J W, KAMPUNZU A B, ARMSTRONG R, YOSHIDA M, OKUDAIRA T, ARIMA M, NGULUBE D A. The Mesoproterozoic Kibaride Belt (Katanga, SE D.R. Congo) [J]. Journal of African Earth Sciences, 2006, 46(1/2): 1−35.

[32] KOKONYANGI J, ARMSTRONG R, KAMPUNZU A B, YOSHIDA M, OKUDAIRA T. U−Pb zircon geochronology and petrology of granitoids from Mitwaba (Katanga, Congo): Implications for the evolution of the Mesoproterozoic Kibaran Belt [J]. Precambrian Research, 2004, 132(1/2): 79−106.

[33] DEWAELE S, HULSBOSCH N, CRYNS Y, BOYCE A, BURGESS R, MUCHEZ P. Geological setting and timing of the world-class Sn, Nb−Ta and Li mineralization of Manono-Kitotolo (Katanga, Democratic Republic of Congo) [J]. Ore Geology Reviews, 2016, 72: 373−390.

[34] LEHMANN B, LAVREAU J. Geochemistry of tin granites from Kivu/Zaire, Rwanda and Burundi [J]. IGCP Project, 1988, 255: 15−18.

[35] de CLERCQ F, MUCHEZ P, DEWAELE S, BOYCE A. The tungsten mineralization at Nyakabingo and Gifurwe (Rwanda): Preliminary results [J]. Geologica Belgica, 2008, 11(4): 251−258.

[36] POHL W, GÜNTHER M A. The origin of Kibaran (late Mid-Proterozoic) tin, tungsten and gold quartz vein deposits in Central Africa: A fluid inclusions study [J]. Mineralium Deposita, 1991, 26(1): 51−59.

[37] WILSON M. Igneous petrogenesis [M]. Dordrecht: Springer, 1989.

[38] RAHMAN A F M. Nature of biotites from alkaline, calc-alkaline, and peraluminous magmas [J]. Journal of Petrology, 1994, 35(2): 525−541.

[39] PEARCE J A, HARRIS N B W, TINDLE A G. Trace element discrimination diagrams for the tectonic interpretation of granitic rocks [J]. Journal of Petrology, 1984, 25(4): 956−983.

[40] PEARCE J A. Role of the sub-continental lithosphere in magma genesis at active continental margins [C]// Continental Basalts and Mantle Xenoliths. Cheshire: Shiva Press Limited, 1983: 230−249.

[41] OLISA O G, OKUNLOLA O A, OMITOGUN A A. Rare metals (Ta−Nb−Sn) mineralization potential of pegmatites of Igangan area, southwestern Nigeria [J]. Journal of Geoscience and Environment Protection, 2018, 6(4): 67−88.

[42] SHAW R A, GOODENOUGH K M, ROBERTS N M W, HORSTWOOD M S A, CHENERY S R, GUNN A G. Petrogenesis of rare-metal pegmatites in high-grade metamorphic terranes: A case study from the Lewisian gneiss complex of north-west Scotland [J]. Precambrian Research, 2016, 281: 338−362.

[43] SYLVESTER P J. Post-collisional strongly peraluminous granites [J]. Lithos, 1998, 45(1/2/3/4): 29−44.

[44] FOSSO TCHUNTE P M, TCHAMENI R, ANDRÉ-MAYER A S, DAKOURE H S, TURLIN F, POUJOL M, NOMO E N, SAHA FOUOTSA A N, ROUER O. Evidence for Nb−Ta occurrences in the syn-tectonic pan-African mayo salah leucogranite (northern Cameroon): Constraints from Nb−Ta oxide mineralogy, geochemistry and U−Pb LA-ICP-MS geochronology on columbite and monazite [J]. Minerals, 2018, 8(5): 188.

[45] WATSON E B, HARRISON T M. Zircon saturation revisited: Temperature and composition effects in a variety of crustal magma types [J]. Earth and Planetary Science Letters, 1983, 64(2): 295−304.

[46] LONDON D. A petrologic assessment of internal zonation in granitic pegmatites [J]. Lithos, 2014, 184/185/186/187: 74−104.

[47] MOROZOVA L N, SOKOLOVA E N, SMIRNOV S Z, BALAGANSKY V V, BAZAI A V. Spodumene from rare-metal pegmatites of the Kolmozero lithium world-class deposit on the Fennoscandian shield: Trace elements and crystal-rich fluid inclusions [J]. Mineralogical Magazine, 2021, 85(2): 149−160.

[48] ČERNÝ P, GOAD B E, HAWTHORNE F, CHAPMAN R. Fractionation trends of the Nb- and Ta-bearing oxide minerals in the Greer Lake pegmatitic granite and its pegmatite aureole, southeastern Manitoba [J]. American Mineralogist, 1986, 71: 501−517.

[49] TAYLOR S R, MCLENNAN S M. The continental crust: Its composition and evolution [J]. The Journal of Geology, 1985, 94(4): 57−72.

[50] LINNEN R L, KEPPLER H. Melt composition control of Zr/Hf fractionation in magmatic processes [J]. Geochimica et Cosmochimica Acta, 2002, 66(18): 3293−3301.

[51] BUCHOLZ C E, SPENCER C J. Strongly peraluminous granites across the Archean−Proterozoic transition [J]. Journal of Petrology, 2019, 60(7): 1299−1348.
[52] ČERNÝ P. Characteristics of pegmatite deposits of tantalum [C]//Lanthanides, Tantalum and Niobium. Berlin: Springer, 1989: 195−239.
[53] SELWAY J B. A review of rare-element (Li−Cs−Ta) pegmatite exploration techniques for the superior Province, Canada, and large worldwide tantalum deposits [J]. Exploration and Mining Geology, 2005, 14(1/2/3/4): 1−30.
[54] KÜSTER D, ROMER R L, TOLESSA D, ZERIHUN D, BHEEMALINGESWARA K, MELCHER F, OBERTHÜR T. The Kenticha rare-element pegmatite, Ethiopia: Internal differentiation, U−Pb age and Ta mineralization [J]. Mineralium Deposita, 2009, 44(7): 723−750.
[55] CERNY P, CHAPMAN R, SIMMONS W B, CHACKOWSKY L E. Niobian rutile from the McGuire granitic pegmatite, Park County, Colorado; solid solution, exsolution, and oxidation [J]. American Mineralogist, 1999, 84(5/6): 754−763.
[56] MÜLLER A, ROMER R L, PEDERSEN R B. The Sveconorwegian pegmatite Province — Thousands of pegmatites without parental granites [J]. The Canadian Mineralogist, 2017, 55(2): 283−315.
[57] CERNY P, ERCIT T S. The classification of granitic pegmatites revisited [J]. The Canadian Mineralogist, 2005, 43(6): 2005−2026.
[58] BRADLEY D C, MCCAULEY A D, STILLINGS L M. Mineral-deposit model for lithium−cesium−tantalum pegmatites [R]. U.S. Geological Survey Scientific Investigations Report, 2017.
[59] HULSBOSCH N. Ore deposits: Origin, exploration and exploitation, geophysical monograph [M]. New York: American Geophysical Union, 2019.
[60] LI Huan, WANG Chong, ZHU Da-peng, JIANG Wei-cheng. Metallogenic environment of skarn-type and vein-type Pb−Zn ore body in the Huangshaping deposit and its implications of deep deposit exploration [J]. The Chinese Journal of Nonferrous Metals, 2023, 33: 630−651.
[61] ZHU Da-peng, LI Huan, JIANG Wei-cheng, WANG Chong, HU Xiao-jun, KONG Hua. Ore-forming environment of Pb−Zn mineralization related to granite porphyry at Huangshaping skarn deposit, Nanling Range, South China [J]. Transactions of Nonferrous Metals Society of China, 2022, 32: 3015−3035.
[62] ZHANG Jun-ke, SHAO Yong-jun, CHEN Ke, TAN Hua-jie, TAN Rui-chang, ZHANG Tian-dong, LIU Zhong-fa. Evidence of fluid evolution of Baoshan Cu−Pb−Zn polymetallic deposit: Constraints from in situ sulfur isotope and trace element compositions of pyrite [J]. Transactions of Nonferrous Metals Society of China, 2021, 31(11): 3530−3548.
[63] REN Tao, LI Huan. Research progress of granite-related tin mineralization [J]. Journal of Central South University (Science and Technology), 2022, 53(2): 514−534. (in Chinese)

稀有金属伟晶岩的地球化学和岩石成因：以刚果(金) Karagwe-Ankole 成矿带 Kivu 地区 Lemera 锡矿床为例

Rub'son N'nahano-Ruhindwa HERITIER[1,2], Moïse LUEMBA[3,4],
李 欢[1], Charles NZOLANG[5], Donat KAMPATA[4,6], Joseph NTIBAHANANA[3,4,7]

1. 中南大学 地球科学与信息物理学院 有色金属成矿预测与地质环境监测教育部重点实验室，长沙 410083；
2. 中国地质大学 地质过程与矿产资源国家重点实验室，北京 100083；
3. 中国石油大学(华东) 地球科学与技术学院，青岛 266580；
4. Faculty of Oil, Gas and New Energies, University of Kinshasa, B. P. 127 Kinshasa XI, D. R. Congo；
5. Official University of Bukavu, Bukavu, South Kivu, D. R. Congo；
6. National Geological Service, Ministry of Mines, Kinshasa, D. R. Congo；
7. Geophysical Research Center, Ministry of Research and Technological Innovation, Kinshasa, D. R. Congo

摘 要：本文报道刚果(金)Karagwe-Ankole 成矿带 Kivu 地区 Lemera 花岗伟晶岩型锡矿床的岩石成因和地球化学研究结果。从露头采集 7 个花岗岩伟晶岩样品，并采用 ICP-MS 和 XRF 光谱法对其进行全岩岩石地球化学分析。花岗伟晶岩具有较高的 Al_2O_3、较低的 Fe_2O_3(T)和 MgO 含量(平均值分别为 12.95%、0.96%和 0.16%，质量分数)，岩石铝饱和指数范围为 1.33~2.05。一些重要稀有金属的丰度以及相关关键参数计算结果如下：Sn((1~138)×10^{-6})、Ta((0.20~0.60)×10^{-6})、Nb((1~8)×10^{-6})、Cs((1.20~3.20)×10^{-6})、Rb((3~223)×10^{-6})、Zr((7~201)×10^{-6})；w(K)/w(Rb) (150~272)；w(K)/w(Cs) (9.06~23.3)，w(Nb)/w(Ta) (3.33~14)。结果表明，Lemera 花岗伟晶岩形成于碰撞后期至后碰撞的构造环境中，由过铝质 S 型花岗岩岩浆结晶而成，岩浆经历了强烈的分离结晶作用。该岩体具有锡和锆的矿化。

关键词：Kibaran 成矿带；Lemera 花岗伟晶岩；锡矿床；S 型花岗岩；分离结晶

(Edited by Wei-ping CHEN)